Available online at www.sciencedirect.com
SCIENCE DIRECT®
Chemical Physics Letters 403 (2005) 287–292
CHEMICAL PHYSICS LETTERS
www.elsevier.com/locate/cplett

ICLAS-VeCSEL and FTS spectroscopies of C_2H_2 between 9000 and 9500 cm^{-1}

Alain Campargue [a,*], Le Wang [b], Peter Cermak [a], Shui-Ming Hu [b]

[a] *Laboratoire de Spectrométrie Physique (associated with CNRS, UMR 5588), Université Joseph Fourier de Grenoble, B.P. 87, 38402 Saint-Martin-d'Hères Cedex, France*

[b] *Hefei National Laboratory for Physical Sciences at Microscale, University of Science and Technology of China, Hefei 230026, China*

Received 29 November 2004; in final form 21 December 2004
Available online 22 January 2005

Abstract

The acetylene absorption spectrum has been recorded between 1.10 and 1.05 μm by Fourier Transform Spectroscopy (FTS) and Intracavity Laser Absorption Spectroscopy (ICLAS) based on a Vertical external Cavity Surface Emitting Laser (VeCSEL). Eleven bands of $^{12}C_2H_2$ were detected, six of them being newly reported. The spectroscopic parameters retrieved from the rovibrational analyses improve significantly the accuracy of parameter values available in the literature. One additional band is assigned to the $^{13}C^{12}CH_2$ isotopologue, present in natural abundance in the sample. Finally, three bands newly detected near 12 300 cm^{-1} by ICLAS based on a Ti:Sapphire are also reported. The vibrational upper states are unambiguously assigned on the basis of the effective Hamiltonian model and the observed and predicted vibrational term values are found in good agreement.

1. Introduction

We have previously reported the analysis of the high energy overtone spectrum of acetylene above 10 000 cm^{-1} by Intracavity Laser Absorption Spectroscopy (ICLAS) based on Ti:sapphire or dyes (see for instance [1,2] and the review of the experimental observations of acetylene levels included in [3]). The aim of the present contribution is to complete these investigations by the study of the 9000–9500 cm^{-1} region. This spectral region shows weak absorption bands which were previously investigated by Fourier Transform Spectroscopy (FTS) [4,5] and by ICLAS based on a Neodymium laser in the 9240–9520 cm^{-1} region [6,7]. However the situation is not satisfactory as the reported observations were obtained in different experimental conditions with either a medium sensitivity or a wavenumber accuracy of the order of 0.01 cm^{-1} or worse. We have then undertaken a combined investigation by FTS and ICLAS based Vertical external Cavity Surface Emitting Lasers (VeCSEL) to improve both the line position accuracy and the sensitivity. ICLAS-VeCSEL is a highly sensitive technique [8,9] which was successfully applied between 8900 and 10 100 cm^{-1} for investigations of the overtone spectra of different molecules such as CO_2 [10], N_2O [9,11,12], H_2S [13] and H_2O [14], with typical detectivity of $\alpha_{min} = 10^{-9}$ cm^{-1}. We have recently reported the observation and analysis of new C_2H_2 and C_2D_2 bands by applying this experimental method in the 9500–10 100 cm^{-1} spectral region [15]. Since then, we could provide a new VeCSEL which allows covering the 8800–9620 cm^{-1} window and then to further investigate the acetylene transparency window lying below the strong $3\nu_3$ manifold centred near 9640 cm^{-1}.

* Corresponding author.
E-mail address: alain.campargue@ujf-grenoble.fr (A. Campargue).

0009-2614/$ - see front matter © 2005 Elsevier B.V. All rights reserved.
doi:10.1016/j.cplett.2004.12.111

2. Experiment

The FTS spectrum was recorded in Hefei with a Bruker IFS 120 HR Fourier-transform spectrometer equipped with a multipass White cell adjusted to its maximum optical path length of 105 m. A tungsten source, a CaF_2 beam splitter and a Ge diode detector were used. The line positions were calibrated using the absorption lines of water (present as an impurity in the cell) given in HITRAN [16]. The unapodized resolution was 0.014 cm^{-1}. The accuracy of the unblended lines recorded with a good signal-to-noise ratio was estimated to be better than 0.001 cm^{-1}. Altogether 2456 scans were co-added to improve the signal-to-noise ratio. An overview of the spectrum recorded with a pressure of 87.6 hPa is presented in Fig. 1.

We used the same experimental set up based on a VeCSEL which has been previously described in details in [8,9]. The newly used structure, with a quantum-well active region made up of GaAs-based semiconductors, was processed at the University of Sheffield. By simply translating the VCSEL sample mounted on a translation stage, the laser emission could be tuned between 8800 and 9620 cm^{-1}. We estimate the sensitivity to be limited to $\alpha_{min} \sim 5 \times 10^{-9}$ cm^{-1} which is not as good as the performances achieved at higher energy [9,11–14] as a consequence of the poorer laser properties of the used VeCSEL. The spectra were recorded with generation times up to 120 μs, leading to equivalent absorption path lengths of the order of 20 km. The spectral resolution was about 0.04 cm^{-1} slightly larger than the Döppler broadening (0.025 cm^{-1} FWHM). Depending on the band intensities, pressures between 15 and 150 hPa were adopted. The spectrum in the region of the Q branch of the Π_u–Σ_g^+ transition centered at 9367.75 is presented in Fig. 2 while Fig. 3 shows the gain in terms of sensitivity achieved by ICLAS around the Q branch of the Π_u–Σ_g^+ at 9408.88 cm^{-1}. The wavenumber calibration procedure of the spectra consists, in a first step, of accurately linearizing the wavenumber scale by using fringes of an étalon recorded for each spectrograph position. Then, for each 10 cm^{-1} wide section, the knowledge of reference line positions allow for an accurate calibration. As far as possible, we used as reference the acetylene line positions measured by FTS (see an example in Fig. 3). In the spectral sections where no lines were detected by FTS, we used H_2O line positions: acetylene and H_2O were successively injected in the intracavity cell and their respective spectra were recorded. We adopted the water line positions as given in [17] as reference. From the comparison of the wavenumber values obtained using independent reference lines, the accuracy of the ICLAS line positions was esti-

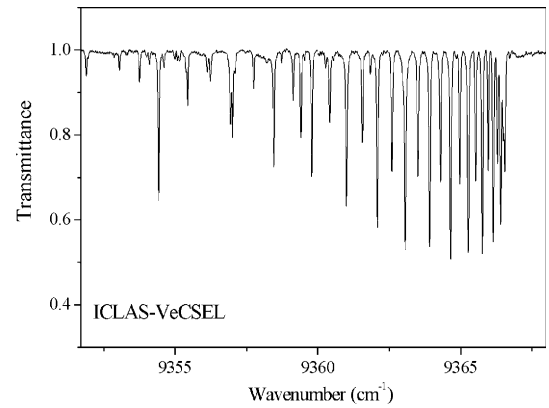

Fig. 2. ICLAS-VeCSEL spectrum of acetylene in the region of the Q branch of the Π_u–Σ_g^+ transition centered at 9367.75 cm^{-1}. The pressure was about 15 hPa and the equivalent absorption pathlength about 12 km.

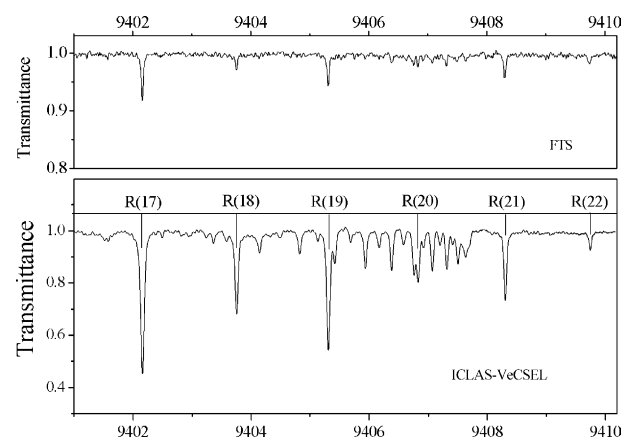

Fig. 3. Comparison of the ICLAS-VeCSEL (P = 52 hPa and $l_{eq} \sim 12$ km) and FTS (P = 87.6 hPa and $l \sim 105$ m) spectra of C_2H_2 in the region of the Q branch of the Π_u–Σ_g^+ transition centered at 9408.87 cm^{-1}. The spectrum includes strong $R(J)$ transitions of the Π_u–Σ_g^+ transition at 9367.75 cm^{-1} which are labeled. The line positions measured on the FTS spectrum were used to calibrate the ICLAS spectrum.

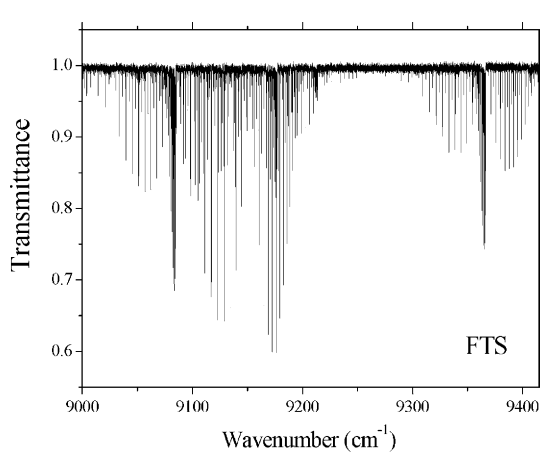

Fig. 1. Overview of the FTS spectrum of acetylene in the 9000–9410 cm^{-1} region recorded with a pressure of 87.6 hPa and a unapodized resolution of 0.014 cm^{-1}.

mated to be around 0.003 cm^{-1} which is not as good as the uncertainty achieved by FTS as a consequence of the indirect procedure required to calibrate the ICLAS spectra.

3. Rotational analysis

Eleven bands were rotationally analyzed between 9000 and 9500 cm^{-1}, six of them being newly detected by ICLAS: the $3\nu_2 + \nu_3$ Σ_u^+–Σ_g^+ band at 9151.73 cm^{-1} accompanied by the Π–Π hot bands from the $\nu_4 = 1$ and $\nu_5 = 1$ bending levels, seven Π_u–Σ_g^+ transitions and a Σ_g^+–Π_u hot band arising from the *e* component levels of the $\nu_5 = 1$ state. After assigning the rotational transitions using the lower state combination differences (GSCD) method, the line positions were fitted on the basis of the standard formula of the energy levels:

$$T_v = G_v(v_1, v_2, v_3, v_4^{l_4}, v_5^{l_5}) + F_v(J), \quad (1)$$

where G_v and F_v are the vibrational and rotational contributions, respectively, with $F_v(J) = B_v[J(J+1) - k^2] - D_v[J(J+1) - k^2]^2$, $k = l_4 + l_5$ being the quantum number associated to the total vibrational angular momentum. The rotational *l*-type doubling contribution to the rotation energy leads to different effective values of the rotational parameters of the *f* and *e* components, which were fitted independently. In the fitting procedure, the rotational constants of the lower state, B'' and D'', were constrained to their literature values [4,18] and the quantities $\tilde{\nu}_0$, ΔB, and ΔD were fitted. The list of the measured wavenumbers with assignments and (obs. − calc) values is attached as Supplementary Material.

Among the six bands newly detected by ICLAS, the Π_u–Σ_g^+ transition at 9213.11 cm^{-1} was also clearly observable in our FTS spectrum. For the bands detected both by FTS and ICLAS, we systematically composed the input dataset by adding to the FTS dataset the wavenumbers of the additional lines detected by ICLAS. By this way, we took fully advantage of the better accuracy of the FTS line positions and of the higher sensitivity of ICLAS. A further reason of not using the ICLAS wavenumbers for the strongest lines is that, in some experimental conditions, their line profiles were observed asymmetric as a consequence of peculiar properties of the VeCSEL laser dynamics (see [19] for more details).

We provide in Table 1 the comparison of the parameter values obtained by using the FTS line positions only, with those obtained with the (FTS + ICLAS) dataset. This Table also gathers the spectroscopic parameters previously obtained by FTS [4,5] and ICLAS-Nd [6,7], showing both the overall agreement and the achieved improvement in the determination of the parameters.

The root mean square deviation of the fits is generally of the order of $1–2 \times 10^{-3}$ cm^{-1} for the FTS datasets and $2–3 \times 10^{-3}$ cm^{-1} for the (FTS + ICLAS) datasets, in agreement with the wavenumber uncertainty. That indicates that the observed rovibrational structures are mostly unperturbed. However, some significant perturbations were clearly observed in particular in the *Q* branch of the Π_u–Σ_g^+ at 9222.168 cm^{-1}, which could not be fitted. Some weak and smooth perturbations may also explain the difference in the vibrational values, G_v, retrieved from the analysis of the *e* and *f* sub bands. For some of the strongest bands the highest *J* transitions could be assigned on the basis of GSCD but their inclusion in the input dataset led to poorer *rms* values even if an higher order term in $H_v[J(J+1) - k^2]^3$ was considered in the expression of the rotational energy. These perturbed transitions which were excluded from the fit, are included in the line lists of the Supplementary Material.

One additional Π–Σ^+ band at 9311.36 cm^{-1} does not show intensity alternation in its rotational structure. It was assigned to the $^{13}C^{12}CH_2$ isotopologue, present in natural abundance (about 2%) in the sample. The results of its spectroscopic analysis are presented in Table 2.

It is worth underlying that many weak lines (up to 50% in some spectral sections) remain unassigned in the ICLAS spectrum, some of them showing regularly spaced structure with an about 2*B* line separation. We believe that part of these transitions are due to hot bands in particular the Δ–Π bands accompanying the strong Π–Σ bands observed at 9086.159 and 9367.73 cm^{-1}.

Finally, we take advantage of the present work to report on three new bands which could be identified between 12 000 and 12 500 cm^{-1} in spectra previously recorded by ICLAS-Ti:Sapphire spectra: the Σ_u^+–Π_g hot band at 12062.81 cm^{-1} and two Σ_u^+–Σ_g^+ bands at 12363.27 and 12383.10 cm^{-1}. These observations complete those we performed by FT-ICLAS in the same spectral region [2]. The corresponding rovibrational parameters are included in Table 1. It is worth mentioning that the rotational structure of the Σ_u^+ level at 12383.10 cm^{-1} is perturbed: we could assign transitions for *J* up to 21 on the basis of GSCD but only transitions with $J < 9$ could be reproduced with a reasonable *rms* value.

4. Vibrational analysis

The effective Hamiltonian model of [20,21] has been showed to successfully reproduce the vibrational energy pattern of $^{12}C_2H_2$ up to the visible region. The complete set of predicted vibrational energies and predicted rotational constants B_v for states up to 15 000 cm^{-1} can be found in [22] together with the exhaustive list of the experimental levels reported in the literature. All the observed vibrational upper states are univocally assigned

Table 1
Rovibrational parameters (in cm^{-1}) of the bands of $^{12}C_2H_2$ detected by FTS and ICLAS-VeCSEL between 9000 and 9500 cm^{-1} and by ICLAS-Ti:Sapphire between 12 000 and 12 400 cm^{-1}

Lower state[a]				G_v	B_v	$D_v \times 10^6$			
(00000) Σ_g^+				0.0	1.176646	1.62710			
(00010) $\Pi_g e$				612.8710	1.175316	1.636			
(00010) $\Pi_g f$				612.8710	1.1805461	1.676			
(00001) $\Pi_u e$				730.3341	1.176432	1.6273			
(00001) $\Pi_u f$				730.3341	1.181132	1.664			
Band type		ΔG_v[b]	v_0[c]	G_v	B_v	$D_v \times 10^6$	J_{MAX} P/Q/R	n/N[d]	$rms \times 103$[e]
Π_u–Σ_g^+	FTS *e*	9086.15251 (37)	9084.99586 (37)		1.1566529 (29)	1.6446 (41)	27/ /27	47/53	1.3
	FTS *f*	9086.15802 (37)	9084.99567 (37)		1.1623522 (51)	1.850 (13)	/20/	20/20	0.8
	ICLAS *e*	9086.15262 (41)	9084.99597 (41)		1.1566523 (26)	1.6450 (29)	30/ /31	56/59	1.6
	ICLAS *f*	Same as FTS						20/25	
	Elid98 ef	*9086.159*			*1.1595*[f]				
Π_g–Π_u	ICLAS *e*	9104.0512 (10)	9104.0758 (10)	9716.922	1.150691 (12)	1.450 (26)	22/ /19	32/36	2.4
	ICLAS *f*	9104.0439 (13)	9104.0682 (13)	9716.915	1.156290 (18)	1.739 (42)	20/ /19	22/36	2.7
Π_u–Σ_g^+	ICLAS *e*	9128.4810 (22)	9127.3224 (22)		1.158561 (54)	1.89 (28)	13/ /12	16/19	2.8
	ICLAS *f*	9128.4812 (23)	9127.3112 (23)		1.170008 (33)	3.698 (95)	/18/	10/16	2.9
Π_g–Π_u	ICLAS *e*	9139.05993 (88)	9139.08446 (88)	9869.394	1.151907 (12)	1.308 (36)	18/ /16	18/19	1.1
	ICLAS *f*	9139.0624 (14)	9139.0869 (14)	9869.396	1.156644 (20)	1.317 (54)	19/ /17	21/21	2.5
Σ_u^+–Σ_g^+	FTS	9151.73113 (33)			1.1523512 (25)	1.5470 (34)	29/ /27	53/53	1.3
	ICLAS	9151.73120 (32)			1.1523506 (24)	1.5461 (32)	29/ /27	55/60	1.3
	Smith88	*9151.732 (3)*			*1.15239 (9)*	*1.7 (1)*			*7.7*
Π_u–Σ_g^+	FTS *e*	9178.52234 (76)	9177.36358 (76)		1.1587520 (73)	1.4381 (14)	21/ /23	33/34	2.0
	FTS *f*	9178.52581 (58)	9177.36190 (58)		1.1639105 (51)	1.6571 (85)	/25/	22/22	1.3
	ICLAS *e*	9178.51950 (67)[g]	9177.36069 (67)		1.158817 (11)	1.764 (39)	27/ /24	47/55	1.9
	ICLAS *f*	9178.52474 (53)[g]	9177.36080 (53)		1.1639382 (85)	1.780 (31)	/26/	26/26	1.1
	Smith88	*9178.524 (4)*	*9177.36 (4)*		*1.1581 (1)*				*14*
Π_u–Σ_g^+	FTS *e*	9214.2752 (17)	9213.1164 (17)		1.1588425 (24)	2.251 (66)	19/ /17	15/15	2.8
	FTS *f*	9214.2750 (13)	9213.1064 (13)		1.1685768 (23)	2.719 (74)	/17/	12/12	1.9
	ICLAS *e*	9214.27320 (73)	9213.11437 (73)		1.1588290 (70)	2.171 (12)	25/ /24	39/42	2.3
	ICLAS *f*	9214.2757 (10)	9213.1072 (10)		1.168554 (12)	2.607 (24)	/22/	21/22	2.3
Π_u–Σ_g^+	ICLAS *e*	9223.3335 (56)	9222.1680 (56)		1.16554 (15)	−2.62(82)	11/ /11	9/14	4.1
	ICLAS *f*	Perturbed					/11/	0/9	
Σ_u^+–Π_g	ICLAS	9222.2927 (86)[h]	9223.4680 (86)	9835.164	1.15793 (22)	3.8 (13)	12/ /10	9/15	3.0
Σ_u^+–Σ_g^+	*Herm89*	*9835.1633* (4)[h]		*9835.163*	*1.157558 (2)*	*1.586 (2)*	*29/ /33*	*61/61*	*1.5*
Π_u–Σ_g^+	FTS *e*	9367.74914 (34)	9366.59223 (34)		1.1569090 (31)	1.6419 (52)	25/ /24	43/44	1.1
	FTS *f*	9367.75528 (62)	9366.59331 (62)		1.1619675 (48)	1.7129 (69)	/27/	25/26	1.5
	ICLAS *e*	9367.74908 (61)	9366.59218 (61)		1.1569086 (36)	1.6310 (38)	33/ /30	62/65	2.5
	ICLAS *f*	9367.75542 (67)	9366.59345 (67)		1.1619692 (29)	1.7166 (22)	/37/	33/34	2.1
	Herm89 ef	*9367.753 (7)*[i]	*9366.596 (7)*		*1.15659 (12)*	*0.05 (41)*	*/17/11*	*13/13*	*9.6*
	Smith88 e	*9367.760 (4)*	*9366.603 (4)*		*1.1566 (1)*				*9.5*
	Smith88 f	*9367.760 (4)*	*9366.598 (4)*		*1.16188 (1)*				*7.6*
	Sini80 e	*9367.75 (1)*	*9366.59 (1)*		*1.1568 (1)*				*29*
	Sini80 f	*9367.73 (2)*	*9366.57 (2)*		*1.1619 (1)*				*13*
	Lopa80 f	*9367.73 (3)*	*9366.597 (3)*		*1.162 (6)*				
Π_u–Σ_g^+	ICLAS *e*	9408.8727 (11)	9407.7132 (11)		1.159480 (26)	2.58 (11)	12/ /14	16/24	2.2
	ICLAS *f*	9408.88537 (73)	9407.71575 (73)		1.1696185 (50)	3.1742 (62)	/29/	26/26	1.9
	Sini80 e	*9408.88 (2)*	*9407.72 (2)*		*1.1592 (4)*				*23*
	Sini80 f	*9408.87 (4)*	*9407.70 (4)*		*1.1700 (3)*				*19*
Σ_u^+–Π_g	ICLAS *e*	12062.8071 (11)	12063.9824 (11)	12675.678	1.151611 (19)	0.926 (67)	17/18/19	37/45	3.1
Σ_u^+–Σ_g^+	*Halo93*	*12675.6769 (40)*	*12675.6769 (40)*	*12675.677*	*1.150961 (42)*	*1.877 (86)*	*37/ /35*	*/74*	
Σ_u^+–Σ_g^+	ICLAS	12363.2709 (22)			1.149120 (27)	3.472 (64)	15/ /21	18/24	4.3
Σ_u^+–Σ_g^+	ICLAS	12383.0988 (27)			1.14833 (16)	16.8 (19)	19/ /21	15/32	6.6

The results obtained in previous studies are given in italics for comparison: Elid98: Ref. [3], Smith88: Ref. [5], Herm89: Ref. [4], Sini80: Ref. [6], Lopa80: Ref. [7], Halo93: Ref. [23].

[a] The lower state rotational constants were taken from [4,18].

[b] Difference of the upper and lower vibrational term values of the transition related to the band center: $\nu_0 = G_v - G_v'' + B''l''^2 - B'l'^2$.

[c] Band center, given only when it differs from ΔG_v.

[d] *n*: number of transitions included in the fit; *N*: number of assigned rotational transitions.

[e] Root mean square deviation of the fit in 10^{-3} cm^{-1} unit.

[f] The *e* and *f* subbands were fitted simultaneously – average values of B^e and B^f.

[g] The H_v constant was included in the fit: H_v (*e*) = 4.21 (39) × 10^{-10} cm^{-1}, H_v (*f*) = 1.34 (31) × 10^{-10} cm^{-1}.

[h] In [4], the parameter values of the upper level were obtained from the analysis of a strong Σ_u^+–Σ_g^+ transition from the ground level, which explains their better determination. Note the good agreement of the upper vibrational term values.

[i] Same as footnote f. q_v = 5.03 (6) × 10^{-3} cm^{-1}.

Table 2
Rovibrational parameters (in cm^{-1}) of the band of $^{12}C^{13}CH_2$ centered at 9331.36 cm^{-1}

		G_v	B_v	$D_v \times 10^6$			
Ground state[a]	(00000) Σ_g^+	0.0	1.148460772	1.556658			
Band type	v_0	G_v	B_v	$D_v \times 10^6$	J_{MAX} $P/Q/R$	n/N	$rms \times 10^3$
Π_u–Σ_g^+e	9311.3606 (12)	9312.4906 (21)	1.129999 (30)	1.55 (10)	16/ /15	14/25	2.4
Π_u–Σ_g^+f	9311.3570 (15)	9312.4930 (15)	1.135989 (49)	3.14 (28)	/13/	11/18	2.6

[a] The ground state rotational constants are from [22].

by comparison with the predictions of this polyad model [21], (see Table 3). The vibrational assignment is provided in terms of the polyad quantum numbers $\{N_s = v_1 + v_2 + v_3, \quad N_r = 5v_1 + 3v_2 + 5v_3 + v_4 + v_5, \quad k = \ell_4 + \ell_5, u/g\}$ to which the states belong to, and in terms of the dominant zero-order vibrational state in their eigenvector expansion.

The seven Π_u levels observed between 9000 and 9500 cm^{-1}, belong to the {3, 14, 1, u} which consists in fifteen levels predicted between 8909 and 9446 cm^{-1} [21] while the Σ_u^+ level at 9151.731 cm^{-1} belongs to the $\{4\ 14\ 0\ u^+\}$ cluster. The upper level of the two hot bands are assigned to different clusters: the Π_g level at 9869.39 cm^{-1} is the first level of the $\{4\ 15\ 1\ g\}$ reported so far while the Π_u level at 9716.92 cm^{-1} is the third level reported for the $\{4\ 15\ 1\ u\}$ cluster (we detected two others around 9930 cm^{-1} as upper levels of Π_u–Σ_g^+ transitions from the vibrational ground state [15]). Finally, the upper level of the Σ_u^+–Π_g hot band at 9835.16 cm^{-1} is a level of the $\{3\ 15\ 0\ u^+\}$ cluster which was previously detected as upper level of a Σ_u^+–Σ_g^+ transition from the ground level [4] (see Table 1). The situation is similar for the Σ_u^+ level of the $\{3\ 15\ 0\ u^+\}$ cluster observed at 12675.678 cm^{-1} through a Σ_u^+–Π_g hot band: it was also observed by excitation from the ground state [23]. The other two Σ_u^+ levels observed by ICLAS-Ti:Sapphire at 12363.27 and 12383.10 cm^{-1} are the first reported levels of the $\{5\ 19\ 0\ u^+\}$ cluster.

The vibrational term values predicted by the effective Hamiltonian model for all the newly observed levels, shows a good agreement with the observations: the maximum deviation is 1.1 cm^{-1} while the average data reproduction of the effective Hamiltonian was $rms = 0.81$ cm^{-1} [21]. As showed in Table 3, the agreement is also satisfactory for the principal rotational constant B_v.

Table 3
Comparison of the experimental and predicted rovibrational parameters of the observed levels of C_2H_2 (in cm^{-1})

Polyad	G_v		B_v		State[b]	Fraction %[c]
	obs.	obs.-pred.	obs.[a]	pred.		
{3 14 1 u}	9086.155	0.5	1.1595	1.159	1111^10^0	89
	9128.481	0.7	1.1643	1.161	1202^21^{-1}	30
	9178.522	0.1	1.1614	1.164	0120^01^1	75
	9214.275	0.3	1.1637	1.164	0211^12^0	53
	9223.334	0.3	1.1655[d]	1.164	0211^12^0	32
					$0211^{-1}2^2$	57
	9367.752	−0.1	1.1594	1.159	2100^01^1	87
	9408.879	−1.3	1.1645	1.165	1200^03^1	82
$\{4\ 14\ 0\ u^+\}$	9151.731	0.4	1.1524	1.152	0310^00^0	97
{4 15 1 u}	9716.919	1.0	1.1535	1.154	0311^10^0	96
$\{3\ 15\ 0\ u^+\}$	9835.164	−0.4	1.1579	1.158	2010^00^0	68
					0030^00^0	30
{4 15 1 g}	9869.395	0.3	1.1543	1.155	0310^01^1	96
$\{5\ 19\ 0\ u^+\}$	12363.271	−0.2	1.1491	1.149	1310^00^0	27
					1401^11^{-1}	52
	12383.099	−1.1	1.1483	1.149	1310^00^0	51
					0501^13^{-1}	46
$\{4\ 20\ 0\ u^+\}$	12675.678	0.7	1.1516	1.152	1030^00^0	71

The calculated values obtained by the effective Hamiltonian model of [21] are tabulated in [3].

[a] The observed values are the average values of B_v^e and B_v^f listed in Table 1.

[b] Dominant zero-order eigenfunctions $(v_1, v_2, v_3, v_4^{l_4}, v_5^{l_5})$ in the composition of the wavefunction of the observed level, as given by the cluster model [21,22].

[c] Square of the coefficient of the dominant state in the eigenvector expansion. Only states with a fraction higher than 25% are mentioned.

[d] Value of B_v^e (B_v^f was not determined).

5. Conclusion

The present contribution illustrates the advantages of combining the spectral information provided by ICLAS and FTS. In spite of the difficulty of absorption experiments in a spectral region where the performances of both techniques are limited by the sharp decrease of the sensitivity of silicon detectors, we could observe eleven bands of $^{12}C_2H_2$ and cover the whole region of the {3, 14, 1, *u*} cluster. Three new bands observed by ICLAS-Ti: sapphire near 12 300 cm^{-1} was also reported. The newly observed levels confirm the good predictive ability of the polyad model of $^{12}C_2H_2$ in the considered energy range.

Acknowledgements

We are indebted to E. Bertseva (Grenoble) for her expert help in the recording of the ICLAS spectra and to J. Vander Auwera (Université Libre de Bruxelles) who provided us the FTS spectrum recorded with a ^{13}C enriched sample of acetylene which confirmed our assignment of the $^{13}C^{12}CH_2$ band. S.-M. Hu acknowledges NFSC for Grant 20103007. A collaborative project between CNRS and CAS is also acknowledged. A. Garnache (CEM2, Université de Montpellier) and J. Roberts (Sheffield, UK) are thanked for providing the *VeCSEL* sample.

Appendix A. Supplementary data

Supplementary data associated with this article can be found, in the online version, at doi:10.1016/j.cplett.2004.12.111.

References

[1] A. Campargue, L. Biennier, M. Herman, Mol. Phys. 93 (1998) 457.
[2] S. Hu, A. Campargue, Z. Wu, Y. Ding, A. Liu, Q. Zhu, Chem. Phys. Lett. 372 (2003) 659.
[3] M. Herman, A. Campargue, M.I. El Idrissi, J. Vander Auwera, J. Phys. Chem. Ref. Data 32 (2003) 921.
[4] M. Herman, T.R. Huet, M. Vervloet, Mol. Phys. 66 (1989) 333.
[5] B.C. Smith, J.S. Winn, J. Chem. Phys. 89 (1988) 4638.
[6] L.N. Sinitsa, J. Mol. Spectrosc. 84 (1980) 57.
[7] V.P. Lopasov, L.N. Sinitsa, A.M. Solodov, Opt. Spectrosc. 49 (1980) 452.
[8] A. Garnache, A.A. Kachanov, F. Stoeckel, R. Houdré, J. Opt. Soc. Am. B 17 (2000) 1589.
[9] E. Bertseva, A.A. Kachanov, A. Campargue, Chem. Phys. Lett. 351 (2002) 18.
[10] Y. Ding, E. Bertseva, A. Campargue, J. Mol. Spectrosc. 212 (2002) 219.
[11] Y. Ding, V.I. Perevalov, S.A. Tashkun, J.-L. Teffo, S. Hu, E. Bertseva, A. Campargue, J. Mol. Spectrosc. 220 (2003) 80.
[12] E. Bertseva, V. Perevalov, S.A. Tashkun, A. Campargue, J. Mol. Spectrosc. 226 (2004) 196.
[13] Y. Ding, O. Naumenko, S. Hu, E. Bertseva, A. Campargue, J. Mol. Spectrosc. 217 (2003) 222.
[14] O. Naumenko, A. Campargue, J. Mol. Spectrosc. 221 (2003) 221.
[15] A. Campargue, E. Bertseva, Yun Ding, J. Mol. Spectrosc. 220 (2003) 13.
[16] L.S. Rothman, A. Barbe, D.C. Benner, L.R. Brown, C. Camy-Peyret, M.R. Carleer, K. Chance, C. Clerbaux, V. Dana, V.M. Devi, A. Fayt, J.-M. Flaud, R.R. Gamache, A. Goldman, D. Jacquemart, K.W. Jucks, W.J. Lafferty, J.-Y. Mandin, S.T. Massie, V. Nemtchinov, D.A. Newnham, A. Perrin, C.P. Rinsland, J. Schroeder, K.M. Smith, M.A.H. Smith, K. Tang, R.A. Toth, J. Vander Auwera, P. Varanasi, K. Yoshino, J. Quant. Spectrosc. Radiat. Transfer 82 (2003) 5.
[17] M.-F. Mérienne, A. Jenouvrier, C. Hermans, A.-C. Vandaele, M. Carleer, C. Clerbauh, P.-F. Coheur, R. Colin, S. Fally, M. Bach, J. Quant. Spectrosc. Radiat. Transfer 82 (2003) 99.
[18] Y. Kabbadj, M. Herman, G. Di Lonardo, L. Fusina, J.W.C. Johns, J. Mol. Spectrosc. 150 (1991) 535.
[19] E. Bertseva, A. Campargue, Opt. Commun. 232 (2004) 251.
[20] M. Abbouti Temsamani, M. Herman, J. Chem. Phys. 102 (1995) 6371.
[21] M.I. El Idrissi, J. Liévin, A. Campargue, M. Herman, J. Chem. Phys. 110 (1999) 2074.
[22] G. Di Lonardo, A. Baldan, G. Bramati, L. Fusina, J. Mol. Spectrosc. 213 (2002) 57.
[23] X. Zhan, L. Halonen, J. Mol. Spectrosc. 160 (1993) 464.